Cdk-mediated phosphorylation of the Kvβ2 auxiliary subunit regulates Kv1 channel axonal targeting

Hélène Vacher,[1,3,4] Jae-Won Yang,[1] Oscar Cerda,[1] Amapola Autillo-Touati,[3,4] Bénédicte Dargent,[3,4] and James S. Trimmer[1,2]

[1]Department of Neurobiology, Physiology, and Behavior, College of Biological Sciences, and [2]Department of Physiology and Membrane Biology, School of Medicine, University of California, Davis, Davis, CA 95616
[3]Institut National de la Santé et de la Recherche Médicale, Unité Mixte de Recherche 641, Marseille 13916, France
[4]Université de la Méditerranée, Institut Fédératif de Recherche 11, Marseille 13916, France

Kv1 channels are concentrated at specific sites in the axonal membrane, where they regulate neuronal excitability. Establishing these distributions requires regulated dissociation of Kv1 channels from the neuronal trafficking machinery and their subsequent insertion into the axonal membrane. We find that the auxiliary Kvβ2 subunit of Kv1 channels purified from brain is phosphorylated on serine residues 9 and 31, and that cyclin-dependent kinase (Cdk)–mediated phosphorylation at these sites negatively regulates the interaction of Kvβ2 with the microtubule plus end–tracking protein EB1. Endogenous Cdks, EB1, and Kvβ2 phosphorylated at serine 31 are colocalized in the axons of cultured hippocampal neurons, with enrichment at the axon initial segment (AIS). Acute inhibition of Cdk activity leads to intracellular accumulation of EB1, Kvβ2, and Kv1 channel subunits within the AIS. These studies reveal a new regulatory mechanism for the targeting of Kv1 complexes to the axonal membrane through the reversible Cdk phosphorylation-dependent binding of Kvβ2 to EB1.

Introduction

Voltage-gated potassium channels of the Kv1 subfamily play an important role in regulating the initiation and the shape of the axonal action potential, as well as synaptic efficiency (Bean, 2007; Clark et al., 2009; Johnston et al., 2010). In addition, mutations in genes encoding Kv1 channel subunits have been implicated in the etiology of several neuronal excitability disorders and diseases (Adelman et al., 1995; Kullmann and Hanna, 2002; Jen et al., 2007). Importantly, Kv1 channel complexes show intricate axonal localizations with regard to their subunit composition and discrete subdomain distributions. For example, in neocortical layer 2/3 pyramidal neurons, in pyramidal neurons in hippocampal CA1, and in retinal ganglion cells, Kv1.1 and Kv1.2 subunits are highly clustered at the distal end of the axon initial segment (AIS) (Inda et al., 2006; Van Wart et al., 2007; Goldberg et al., 2008; Lorincz and Nusser, 2008). In the case of myelinated nerve fibers, Kv1 channels are restricted beneath the myelin sheath and flanking each node of Ranvier at sites termed juxtaparanodes (Wang et al., 1993; Rhodes et al., 1995; Rasband, 2004). However, the mechanisms underlying the precise assembly of high density populations of Kv1 channels in distinct axonal membrane subdomains remain elusive.

Kv1 channels function as supramolecular protein complexes, composed of four pore-forming and voltage-sensing principal, or α, subunits, with four cytoplasmic auxiliary Kvβ subunits (Rhodes et al., 1996; Pongs et al., 1999; Long et al., 2005). These Kv1α (Kv1.1–1.8) and Kvβ (Kvβ1, Kvβ2) subunits can heteromultimerize to yield biophysically and pharmacologically distinct channel complexes (Ruppersberg et al., 1990; Rettig et al., 1994; Xu et al., 1998). Auxiliary Kvβ subunits are each ∼300 amino acids in length and contain a unique N-terminal domain followed by a common conserved core (over 85% amino acid identity; Trimmer, 1998). Studies of Kv1 channel biosynthesis have shown that Kv1α and Kvβ subunits coassemble in the ER and remain together as a stable complex (Shi et al., 1996;

Correspondence to Helene Vacher: helene.vacher@univmed.fr

J.-W. Yang's present address is Medical University of Vienna, Institute of Pharmacology, A-1090 Vienna, Austria.

Abbreviations used in this paper: +TIP, microtubule plus end–tracking protein; AIS, axon initial segment; Ank-G, ankyrin-G; APC, adenomatous polyposis coli; API, axonal polarity index; CLASP, CLIP-associated protein; DIV, days in vitro; LC-MS/MS, liquid chromatography tandem mass spectrometry; MT, microtubule; phosphosite, phosphorylation site; WT, wild type.

The Rockefeller University Press $30.00
J. Cell Biol. Vol. 192 No. 5 813–824
www.jcb.org/cgi/doi/10.1083/jcb.201007113

Nagaya and Papazian, 1997). Kvβ subunits primarily attach to the tetramerization or T1 domain present on the cytoplasmic N termini of Kv1α subunits (Sewing et al., 1996; Gulbis et al., 2000; Long et al., 2005). Cryo-electron microscopy (Orlova et al., 2003; Sokolova et al., 2003) and x-ray crystallography (Gulbis et al., 1999, 2000; Long et al., 2005) studies of the Kv1/Kvβ channel complex place the Kvβ subunits as a large cytoplasmic mass hanging well beneath the cytoplasmic face of the pore module of Kv1 channels. Compelling data demonstrate that cytoplasmic Kvβ2 subunits, which do not dramatically affect the inactivation of Kv1 channels as do Kvβ1 subunits (Rettig et al., 1994), are the predominant Kvβ subunit in mammalian brain (Rhodes et al., 1996). Kvβ2 is involved in ER export of Kv1 channels (Shi et al., 1996; Nagaya and Papazian, 1997; Campomanes et al., 2002) and controls Kv1 channel axonal targeting via its interaction with the microtubule plus end–tracking protein (+TIP) EB1 (Gu et al., 2003, 2006). The microtubule-based motor KIF3/ kinesin II and KIF5B are also implicated in Kv1 axonal targeting (Gu et al., 2006; Rivera et al., 2007). EB1 and its family members autonomously track microtubule tips, most likely by recognizing structural features of growing microtubule ends (Bieling et al., 2007; Vitre et al., 2008; Dixit et al., 2009). The C-terminal moiety of EB1 is described as an important domain for mediating EB1 binding to an array of structurally and functionally unrelated +TIP-binding partners, such as the adenomatous polyposis coli (APC) tumor suppressor protein and CLIP-associated proteins (CLASPs; Honnappa et al., 2005, 2009). Phosphorylation of a number of these EB1-binding proteins negatively regulates their association with EB1 (Honnappa et al., 2009; Kumar et al., 2009). As Kvβ2 is a stable, component subunit of Kv1 channel complexes (Shi et al., 1996; Nagaya and Papazian, 1997), the regulated dissociation of Kvβ2 from the channel complexes does not appear to be a viable mechanism for separating Kv1 channel complexes from EB1 and microtubules (MTs). This raised questions as to whether Kvβ2–EB1 interaction itself could be dynamically regulated through phosphorylation, and consequently modulate the targeting of Kv1 channels to specific sites in axons. Here we identified novel in vivo phosphorylation sites (phosphosites) on Kvβ2. Our functional analysis of the role of phosphorylation at these sites shows that Kvβ2–EB1 interaction is negatively regulated by Cdk-mediated phosphorylation, and that Kvβ2 phosphorylation is critical in regulating the axonal targeting of Kv1-containing Kv channels.

Results

Identification of in vivo phosphosites on brain Kvβ2

To identify in vivo Kvβ2 phosphosites, we undertook an unbiased liquid chromatography tandem mass spectrometry (LC-MS/MS)–based analysis of Kvβ2 subunits immunopurified from mammalian brain. To specifically isolate the population of brain Kvβ2 associated with Kv1 channels, we used an anti-Kv1.2 antibody (Ab) to coimmunopurify Kv1/Kvβ2 complexes from detergent extracts of a crude rat brain membrane (RBM) fraction. We then size-fractionated the components of the purified

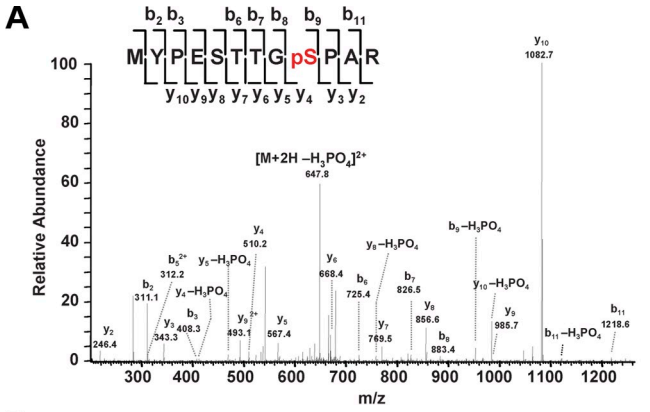

B

```
  1 MYPESTTGSP ARLSLRQTGS PGMIYSTRYG SPKRQLQFYR
 41 NLGKSGLRVS CLGLGTWVTF GGQITDEMAE HLMTLAYDNG
 81 INLFDTAEVY AAGKAEVVLG NIIKKKGWRR SSLVITTKIF
121 WGGKAETERG LSRKHIIEGL KASLERLQLE YVDVVFANRP
161 DPNTPMEETV RAMTHVINQG MAMYWGTSRW SSMEIMEAYS
201 VARQFNLIPP ICEQAEYHMF QREKVEVQLP ELFHKIGVGA
241 MTWSPLACGI VSGKYDSGIP PYSRASLKGY QWLKDKILSE
281 EGRRQQAKLK ELQAIAERLG CTLPQLAIAW CLRNEGVSSV
321 LLGASNAEQL MENIGAIQVL PKLSSSIVHE IDSILGNKPY
361 SKKDYRS
```

Figure 1. **In vivo phosphosites on mammalian brain Kvβ2.** (A) Identification of phosphosites on rat brain Kvβ2 using LC-MS/MS. A doubly charged, singly phosphorylated peptide at *m/z* 647.8, derived from Kvβ2 purified from rat brain, was fragmented to produce this MS/MS spectrum with a *y*- and *b*-ion series that described the sequence MYPESTTGpSPAR (aa 1–12). The phosphosite was unambiguously assigned to Ser9 because of mass assignments from β-eliminated y_4, y_5, y_8, y_{10}, b_9, and b_{11} fragment ions with neutral loss of phosphoric acid H_3PO_4. (B) Deduced amino acid sequence of rat Kvβ2. Phosphorylated serine residues, identified by MS, are in red. The sequence coverage is indicated in bold.

complexes by SDS-PAGE. The Coomassie blue–stained band representing the putative Kvβ2 subunit pool of $M_r \approx 40$ kD was excised and subjected to in-gel trypsin digestion. Peptides were fractionated and identified using LC-MS/MS. A Mascot database search of identified mass spectra resulted in 437 matched peptides and 79% overall coverage of the Kvβ2 primary sequence (Fig. 1). From these analyses, four phosphorylated amino acids were unambiguously identified: phosphoserines at S9 (TTGpSPAR), S20 (QTGpSPGM), S31 (TRYGpSPKR), and S112 (WRRSpSLVIT; Fig. 1 and Table I). Using this same approach, we also unambiguously identified the S20 and S112 phosphosites on Kvβ2 copurified with Kv1.2 from extracts of mouse brain, and pS31 and pS112 from extracts of human hippocampus (Table I). The pS9, pS20, and pS31 sites are present on the unique N terminus of Kvβ2 (aa 1–38). In contrast, pS112 is present within the core domain that is highly conserved among all Kvβ subunits, and the tryptic peptide containing this site (GWRRSpSLVITTK) is 100% identical in Kvβ1. However, as no peptides unique to Kvβ1 were identified in these analyses, we assume the peptide containing pS112 originated from Kvβ2. These data show that Kvβ2 is phosphorylated in a similar but not identical pattern when purified from rat, human, and mouse brain. Note that recent high throughput mouse brain phosphoproteomic studies have provided evidence for Kvβ2 phosphorylation at S9, S20, and S112 (Baek et al., 2011).

Table I. **LC-MS/MS identification of in vivo phosphosites on Kvβ2 purified from brain**

Phosphorylation site	Native		
	Rat brain	Mouse brain	Human HC
pS9	+	−	−
pS20	+	+	−
pS31	+	−	+
pS112	+	+	+

HC, hippocampus; +, identified phosphorylation site; −, phosphorylation site not identified.

Impact of S9 and S31 Kvβ2 mutations on Kv1 channel axonal targeting in neurons

Previous studies showed that Kvβ auxiliary subunits and Kv1 subunits coassemble before the resultant $\alpha_4\beta_4$ channel complexes exit the ER (Shi et al., 1996; Nagaya and Papazian, 1997) and that Kvβ2 association is crucial for efficient cell surface trafficking of Kv1.2 (Shi et al., 1996; Campomanes et al., 2002). To determine if any of the identified Kvβ2 phosphosites are involved in cell surface trafficking of Kv1.2, we replaced the phosphorylated Ser residues with Ala residues. We first looked at the effect of these phosphosite mutations on the cell surface expression of Kv1.2 using immunostaining with an ectodomain-directed anti-Kv1.2 Ab (Kv1.2e). Coexpression of Kv1.2 with the S9A, S31A, and S9A/S31A mutants in COS-1 cells led to a decrease of the number of cells exhibiting cell surface immunostaining for Kv1.2, when compared with coexpression with wild-type (WT) Kvβ2, or with the S20A and S112A mutants (Fig. 2 A). We also observed a significant reduction in Kv1.2 ionic currents in whole-cell patch-clamp recordings of HEK293 cells expressing either S31A (Fig. 2 B) or S9A (not depicted), when compared with cells expressing WT Kvβ2 (Fig. 2 B) or S20A (not depicted). The macroscopic voltage-dependent activation and inactivation gating characteristics of Kv1.2 were not detectably different in cells coexpressing mutant and WT Kvβ2. Together, these results indicate that phosphorylation at S9 and S31 is involved in regulating cell surface expression levels of Kv1.2, presumably due to effects on intracellular trafficking.

In hippocampal neurons in culture, Kvβ2 mediates the polarized targeting of Kv1 channel complexes to axons (Gu et al., 2003). We next asked whether mutating Kvβ2 phosphosites would affect the polarized expression of Kv1.2 in axons. Rat hippocampal neurons in culture were cotransfected at 7 days in vitro (DIV), a time before the expression of endogenous Kv1α subunits and Kvβ2 (Gu et al., 2006), with Kv1.2 and WT or mutant isoforms of Kvβ2, and the localization of cell surface Kv1.2 determined 2–3 d later. Intact neurons were immunostained with the external Kv1.2e Ab to detect surface Kv1.2, and then permeabilized and immunostained to determine the localization of the overall population of WT and mutant cytoplasmic Kvβ2 subunits (Fig. 2 C). To quantify the polarity of the expression of cell surface Kv1.2, we determined the surface axonal polarity index (API), defined as the ratio of average fluorescence intensity for major axonal to dendritic branches (Gu et al., 2003). As previously shown (Gu et al., 2003), cell surface Kv1.2 exhibited a nonpolarized surface distribution when expressed in the absence of Kvβ2 (Fig. 2 D; API = 0.74 ± 0.17, n = 13), and a highly polarized axonal surface distribution when coexpressed with Kvβ2 (Fig. 2 D; API = 1.90 ± 0.35, n = 17; significantly [$P < 0.05$] different than with no Kvβ2). In contrast, when Kv1.2 was coexpressed with either the S9A or S31A mutant, it exhibited a nonpolarized surface distribution similar to that observed in the absence of Kvβ2 (Fig. 2 D; API = 0.73 ± 0.21, n = 14; and API = 0.73 ± 0.23, n = 14, respectively, not significantly different than with no Kvβ2). Moreover, the expression of S9A/S31A in mature neurons (e.g., endogenously expressing Kv1 channels and Kvβ2) also led to a decrease in the axonal distribution of endogenous Kv1.2 (Fig. S2). Together, these results indicate that Kvβ2 S9 and S31 are crucial to both the intracellular trafficking of Kv1.2 to the cell surface and the axonal localization of cell surface Kv1.2.

Although none of the identified phosphosites are located in the region of Kvβ2 that serves as the primary mediator of its interaction with Kv1.2 (Gulbis et al., 2000; Long et al., 2005), we nonetheless determined experimentally whether mutations at these sites could impact Kv1.2 trafficking by simply disrupting the interaction of Kvβ2 with Kv1.2. We performed reciprocal coimmunoprecipitation experiments from coexpressing COS-1 cells, and found that both WT and mutant Kvβ2 subunits were associated with Kv1.2 (Fig. 2 E), and vice versa (not depicted). Anti-Kvβ2 Abs did not directly immunoprecipitate Kv1.2 (Fig. 2 E), and anti-Kv1.2 Abs did not immunoprecipitate Kvβ2 (not depicted). These results suggest that the negative impact of the S9A and S31A mutations on the intracellular trafficking and axonal localization of cell surface Kv1.2 are due to events subsequent to Kv1.2/Kvβ2 assembly.

Kvβ2 S9 and S31 are key residues in modulating the interaction of Kvβ2 with EB1

A previous study showed that axonal targeting of Kv1.2 is dependent on the direct interaction of Kvβ2 with EB1, and that Kvβ2 associates with the EB1 C terminus via interactions requiring intact Kvβ2 N-terminal (aa 1–90) and C-terminal (aa 338–367) domains (Gu et al., 2006). The model that arose from these studies is that association of Kvβ2 with EB1 enables the recruitment of Kv1–Kvβ2 complexes to MTs, allowing for the transport of these complexes to the axon (Gu et al., 2006). To determine whether the disruption of Kvβ2-mediated Kv1.2 axonal compartmentalization by the S9A and S31A mutations was due to a perturbation of interaction with EB1, we first examined the recruitment of these Kvβ2 phosphosite mutants along

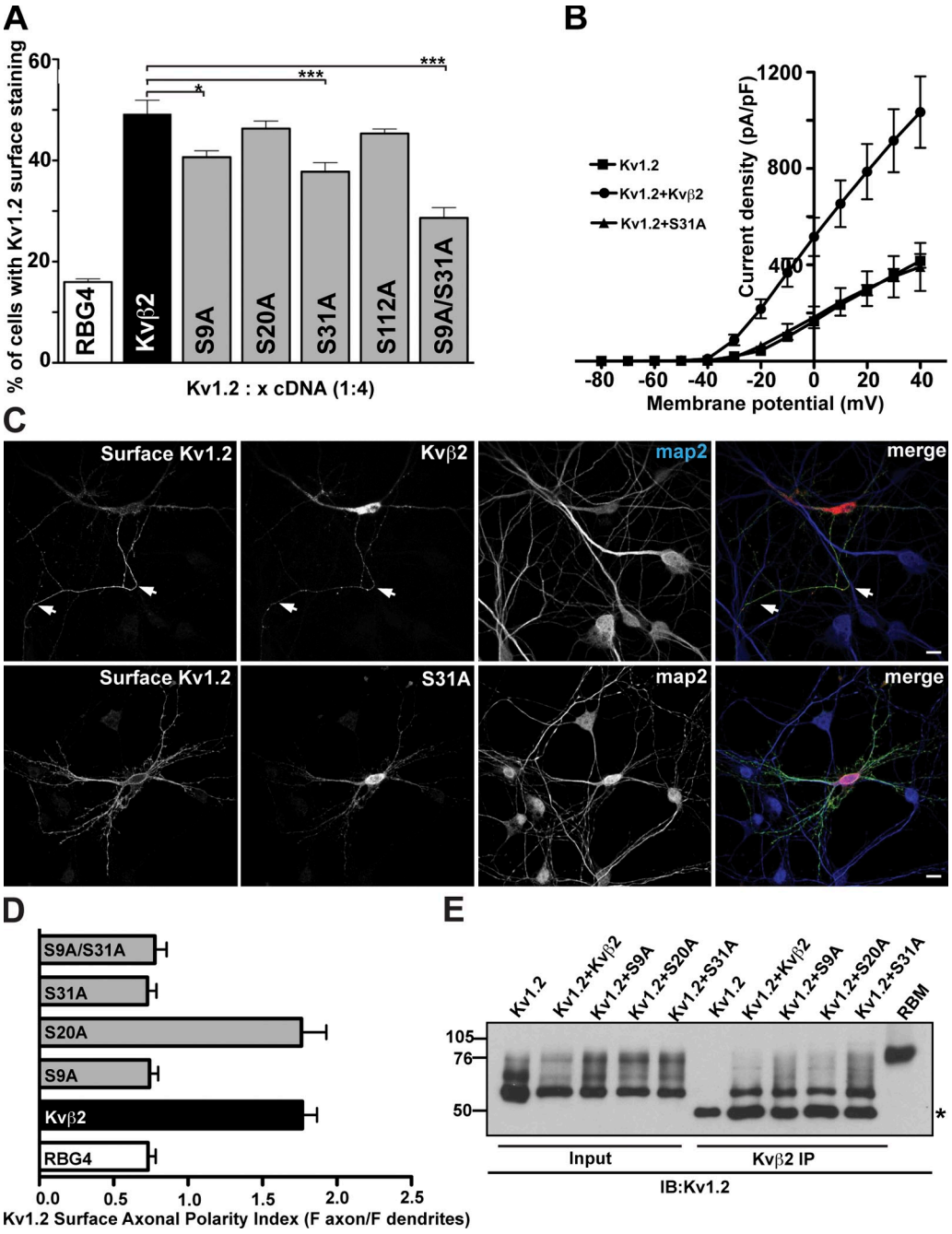

Figure 2. **Mutating Kvβ2 N-terminal phosphosites impacts Kv1.2 cell surface expression.** (A) Intact COS-1 cells cotransfected with rat Kv1.2 and WT Kvβ2, or Kvβ2 mutants (S9A, S20A, S31A, S112A, and S9A/S31A) were double immunostained with external Kv1.2e Ab, followed by permeabilization and immunostaining with K14/16 mAb. A surface expression efficiency index was determined as the percentage of Kv1.2-expressing (K14/16-positive) cells that exhibited Kv1.2e surface immunostaining (Kv1.2 + Kvβ2 = 49.2 ± 2.7%; Kv1.2 + S9A = 40.7 ± 1.2%; Kv1.2 + S31A = 37.8 ± 1.8%; and Kv1.2 + S9A/S31A = 28.7 ± 12.0%). Statistical significance was determined by one-way ANOVA followed by Tukey's post hoc test and statistical significance was considered at: *, $P < 0.05$; and ***, $P < 0.001$ ($n = 6$ experiments of 100 Kv1.2-positive cells counted per experiment). (B) Whole-cell patch-clamp recordings from HEK293 cells expressing rat Kv1.2 alone (squares), or Kv1.2 together with WT Kvβ2 (circles), or the Kvβ2 S31A mutant (triangles). The cells were held at −80 mV and step depolarized to +40 mV for 200 ms in +10-mV increments. Peak current amplitudes at each test potential were divided by the cell capacitance to obtain the current densities. Mean ± SE of current densities obtained (Kv1.2, $n = 14$; Kv1.2 + Kvβ2, $n = 5$; Kv1.2 + S31A, $n = 5$) were plotted against each test potential. (C) Cultured hippocampal neurons (7 DIV) were cotransfected with Kv1.2 and either WT Kvβ2 or Kvβ2 S31A. 2 d after transfection, intact neurons were immunostained with Kv1.2e Ab, and then permeabilized and immunostained with anti-Kvβ2 and anti-MAP2 Abs. White arrows indicate the axon. Bar, 50 µm. (D) Surface axonal polarity index was determined by quantifying the surface immunofluorescence intensity profiles of the axon versus three dendritic branches using NIH Neuron/J. (E) Coimmunoprecipitation assays from heterologous cells coexpressing Kvβ2 mutants and Kv1.2 channels. Input into and products of immunoprecipitation reactions performed with anti-Kvβ2 mAb K25/73 on lysates from COS-1 cells coexpressing Kv1.2 and WT Kvβ2 or Kvβ2 mutants (S9A, S20A, or S31A), and immunoblotted for Kv1.2 using K14/16. Asterisk indicates the mouse IgG band. Input and IP lanes are not normalized.

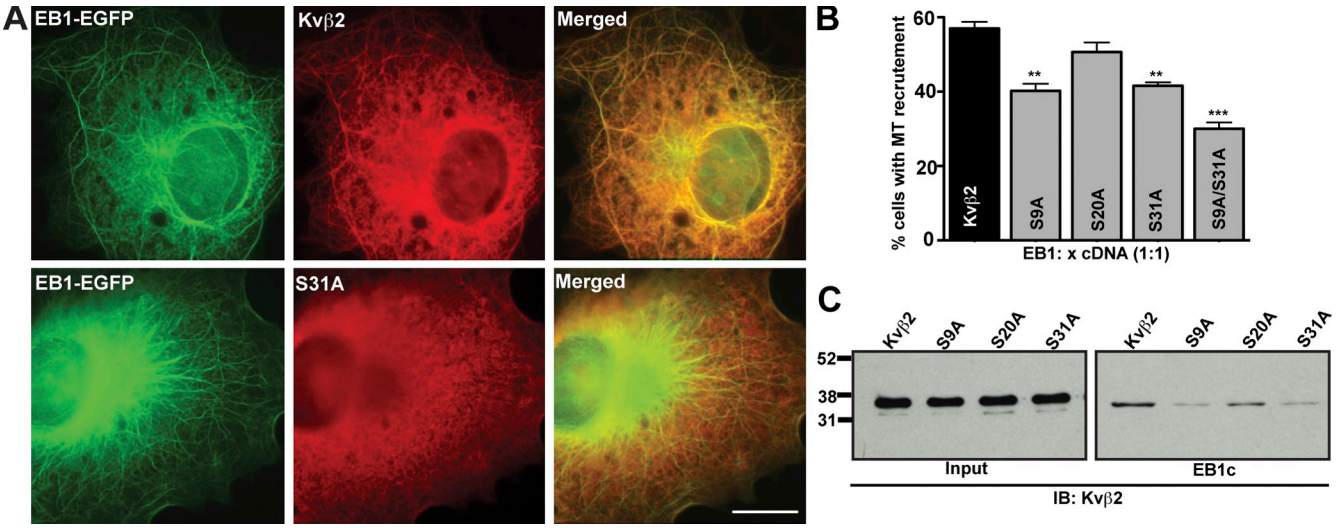

Figure 3. **Mutating Kvβ2 N-terminal phosphosites impacts Kvβ2–EB1 interaction.** (A) COS-1 cells cotransfected with EB1-EGFP and WT Kvβ2, or Kvβ2 S31A (ratio 1:1). After methanol fixation, cells were immunostained with anti-Kvβ2 mAb K25/73 (red). Bar, 20 µm. (B) MT recruitment was quantified by dividing the number of cells with MT-like Kvβ2 immunostaining by the total number of cells coexpressing Kvβ2 and EB1; 500 cells were counted from three independent experiments. **, P < 0.01; ***, P < 0.001. (C) GST pull-down assays. Input and products of reactions performed with GST-EB1c on lysates from HEK293 cells expressing WT Kvβ2, or Kvβ2 mutants (S9A, S20A, or S31A) and immunoblotted with an anti-Kvβ2 mAb K25/73.

MTs in the presence of EB1. As previously shown (Nakahira et al., 1998; Campomanes et al., 2002), we observed that Kvβ2 expressed in COS-1 cells is present uniformly throughout the cytoplasm, whereas EB1-EGFP is mainly found along MTs (Skube et al., 2010; unpublished data). However, coexpression of EB1-EGFP promoted the recruitment of Kvβ2 to MTs in 57.0 ± 4.0% (n = 500 cells, three independent experiments) of cotransfected cells (Fig. 3). In contrast, the EB1-dependent MT recruitment of the S9A (40.2 ± 4.3%), S31A (41.6 ± 2.0%), and S9A/S31A (30.0 ± 3.0%) mutants was significantly decreased versus that observed for WT Kvβ2 (n = 500 cells, three independent experiments; Fig. 3). To address whether these effects were due to differences in EB1 binding, we performed GST pull-down assays, similar to those used previously to demonstrate Kvβ2–EB1 interaction (Gu et al., 2006), using bacterially expressed GST-EB1C (C-terminal domain, 165–268) and Kvβ2 expressed in COS-1 cells. As shown in Fig. 3 C, the S9A and S31A mutants were deficient in EB1C binding relative to WT Kvβ2. These findings suggest that S9 and S31 are involved in regulating the association of Kvβ2 with EB1, and the EB1-mediated association of Kvβ2-containing channels with MTs.

Cdk phosphorylation negatively regulates the interaction between Kvβ2 and EB1

The interaction of EB1 with APC (Honnappa et al., 2005) and CLASP2 (Watanabe et al., 2009) is regulated through changes in phosphorylation state of these EB1 binding partners. As our mutagenesis results suggested that mutating Kvβ2 S9 and S31 phosphosites altered Kvβ2 binding to EB1, we next determined whether Kvβ2 phosphorylation could modulate its interaction with EB1. We subjected cell extracts containing Kvβ2 (which is phosphorylated in heterologous cells; see Fig. S1) to digestion with alkaline phosphatase, and then subjected the extracts to pull-down assays with GST-EB1C (see previous paragraph). Our results show that dephosphorylation of Kvβ2 greatly enhances its binding to EB1 (Fig. 4 A), suggesting that phosphorylation of Kvβ2 also negatively regulates its binding to EB1. To determine which protein kinases could regulate Kvβ2–EB1 interaction, we used consensus site algorithms to analyze the sequences surrounding S9 and S31 phosphosites. These in silico analyses revealed a match for both S9 (pSPAR) and S31 (pSPKR) phosphosites with the consensus motif [(S/T)PX(R/K)] for Cdk phosphorylation, specifically that catalyzed by Cdk2 and Cdk5. To examine the possibility that Cdk-mediated phosphorylation regulated Kvβ2–EB1 interaction, we cotransfected Kvβ2 in COS-1 cells with active (Cdk2-HA) or dominant-negative (D146N, Cdk2-DN) versions of Cdk2. GST-EB1C pull-down assays were then performed on the extracts obtained from these cells. The presence of Cdk2-HA abrogated the binding of Kvβ2 to EB1, an effect that was not observed with Cdk2-DN (Fig. 4 B). We next used a phosphospecific Ab specific for Kvβ2 phosphorylated at S31 ("Kvβ2P"; Fig. S1, B and C) to probe blots of bacterially expressed Kvβ2 that had been phosphorylated in vitro by either Cdk2/cyclin A or Cdk5/p35 purified complexes. Phosphospecific Kvβ2P immunoreactivity against Kvβ2 was detected in the reactions performed with either Cdk2/cyclin A or Cdk5/p35 (Fig. 4 C), showing that Kvβ2 could be directly phosphorylated by these Cdks. Together, these results show that Kvβ2–EB1 interaction is regulated by Cdk-mediated phosphorylation of Kvβ2 at the S31 phosphosite, and perhaps by phosphorylation at other sites (e.g., S9) as well.

Cdk inhibition increases Kvβ2 recruitment to MTs and consequently decreases Kv1 surface expression

To better understand the impact of Cdks on Kvβ2 properties, we first tested the impact of the pharmacological inhibition of Cdks on the recruitment of Kvβ2 to MTs. We treated COS-1 cells coexpressing Kvβ2 and EB1 for 24 h with roscovitine, an inhibitor of Cdk kinases (Cdk1, Cdk2, and Cdk5; Bach et al., 2005).

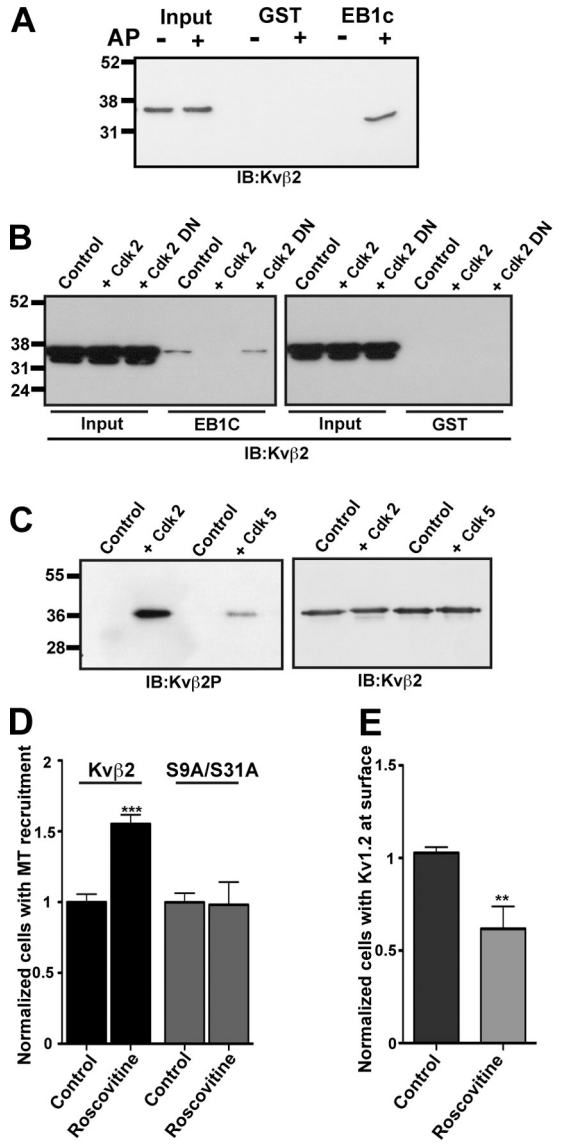

Figure 4. **Cdks regulate the interaction between Kvβ2 and EB1.** (A) Effect of Kvβ2 phosphorylation on its interaction with EB1. Input and products of GST pull-down reactions performed with GST-EB1c on control and alkaline phosphatase–treated Kvβ2 lysates. GST was used as a negative control. The gel was blotted with anti-Kvβ2 mAb K25/73. (B) Role of Cdk2 in regulating Kvβ2–EB1 interaction. Input and products of GST-EB1c pull-down reactions performed on HEK293 lysates expressing Kvβ2 and either Cdk2-HA or Cdk2-DN, and blotted with an anti-Kvβ2 mAb K25/73. The control lane contains a GST-EB1c pull-down performed from HEK293 lysates expressing Kvβ2 alone. (C) Immunoblots of bacterially expressed Kvβ2 phosphorylated in vitro in reactions containing no protein kinase addition (control), or purified human recombinant protein kinase complexes Cdk2/cyclin A, or Cdk5/p35, using the phosphospecific Ab Kvβ2P or anti-Kvβ2 mAb K25/73. (D) Effect of Cdk inhibition on the recruitment of Kvβ2 to MTs. COS-1 cells were cotransfected with EB1-EGFP and WT Kvβ2, or Kvβ2 S9A/S31A (ratio 1:1). After the transfection (i.e., subsequent to Kv1.2/Kvβ2 expression and assembly), cells were treated with 20 µM roscovitine for 24 h. MT recruitment was quantified by dividing the number of cells with MT-like Kvβ2 immunostaining by the total number of cells coexpressing Kvβ2 and EB1; 500 cells were counted from three independent experiments. ***, $P < 0.001$. (E) Effect of Cdk inhibition on Kv1.2 surface expression. COS-1 cells were cotransfected with WT Kv1.2 and Kvβ2 (ratio 1:4). After the transfection, cells were treated with 20 µM of roscovitine for 24 h. Intact COS-1 cells were double immunostained with external Kv1.2e Ab, and then after permeabilization with cytoplasmic anti-Kv1.2 K14/16 and anti-Kvβ2 K25/73 mAbs. A surface expression efficiency index was determined as the percentage of Kv1.2-expressing (K14/16-positive) cells with Kv1.2e surface immunostaining. Statistical significance was considered at **, $P < 0.01$. ($n = 3$ independent experiments of 100 Kv1.2-positive cells counted per experiment).

The inhibition of Cdks dramatically increased the recruitment of Kvβ2 to MTs (Fig. 4 D). Importantly, inhibition of Cdks did not affect the MT recruitment of the S9A/S31A mutant, demonstrating that the effects are mediated through Cdk phosphorylation of S9 and S31. We next looked at the effect of Cdk inhibition on the cell surface expression of Kv1.2. Roscovitine treatment of COS-1 cells coexpressing Kv1.2 and Kvβ2 led to a decrease of the number of cells exhibiting cell surface immunostaining for Kv1.2 (Fig. 4 E). Together, these results suggest that Cdk-mediated phosphorylation of Kvβ2 releases Kv1–Kvβ2 complexes from MTs, allowing for their expression in the plasma membrane, by disrupting Kvβ2 interaction with EB1.

Cdks and phosphorylated Kvβ2 colocalize with neuronal Kv1 complexes in vitro and in vivo

In brain, Kv1 channel complexes are found predominantly localized to axons, where they show discrete cell type–dependent localization within subdomains of the axonal membrane (Wang et al., 1993; Rhodes et al., 1997; Lorincz and Nusser, 2008; Ogawa et al., 2008). Given the role of Cdks in mediating Kvβ2–EB1 association revealed in the studies presented in the previous paragraph, we first examined the localization of Kvβ2 phosphorylated at S31 using the phosphospecific Kvβ2P Ab to immunostain rat hippocampal neurons in culture. As the developmental expression of Kv1 complexes in cultured hippocampal neurons begins after 2 weeks of culture (Gu et al., 2006), we used hippocampal neurons at 3 weeks in culture (21 DIV) for these experiments. In these neurons, we observed Kvβ2P immunostaining in the axon, with a high concentration at the AIS (identified by ankyrin-G [Ank-G] immunostaining), and colocalizing extensively with the overall pools of Kvβ2 (Fig. 4 A) and Kv1.2 (not depicted). Note that Kvβ2P also exhibited additional nuclear immunostaining that appeared to be nonspecific as it did not correspond to immunostaining for Kvβ2. Although Cdk2 immunostaining was broadly distributed throughout these cultured neurons, double immunostaining for Cdk2 and Kvβ2 revealed these proteins colocalized in the axon, and specifically at the AIS (Fig. 5 A). Similarly, immunostaining for Cdk5, which was also broadly expressed in both somatodendritic and axonal compartments, exhibited a prominent colocalization with Kvβ2 at the AIS (Fig. 5 A). To extend these results obtained in cultured neurons, we next used immunostaining to examine the in vivo distribution of Cdks in myelinated axons, where Kv1 channels are highly enriched at the juxtaparanode (Rasband, 2004). The localization of Cdks in axons was assessed on sciatic nerve sections, which have been used previously to define the juxtaparanodal localization of Kv1α subunits (Mi et al., 1995; Rasband et al., 1998) and Kvβ2 (Vabnick et al., 1999). In adult mouse sciatic nerve, Cdk2 immunostaining colocalized with that for Kv1.2 at the juxtaparanode, and was also present at the node of Ranvier (Fig. 5 B). Cdk5 immunostaining

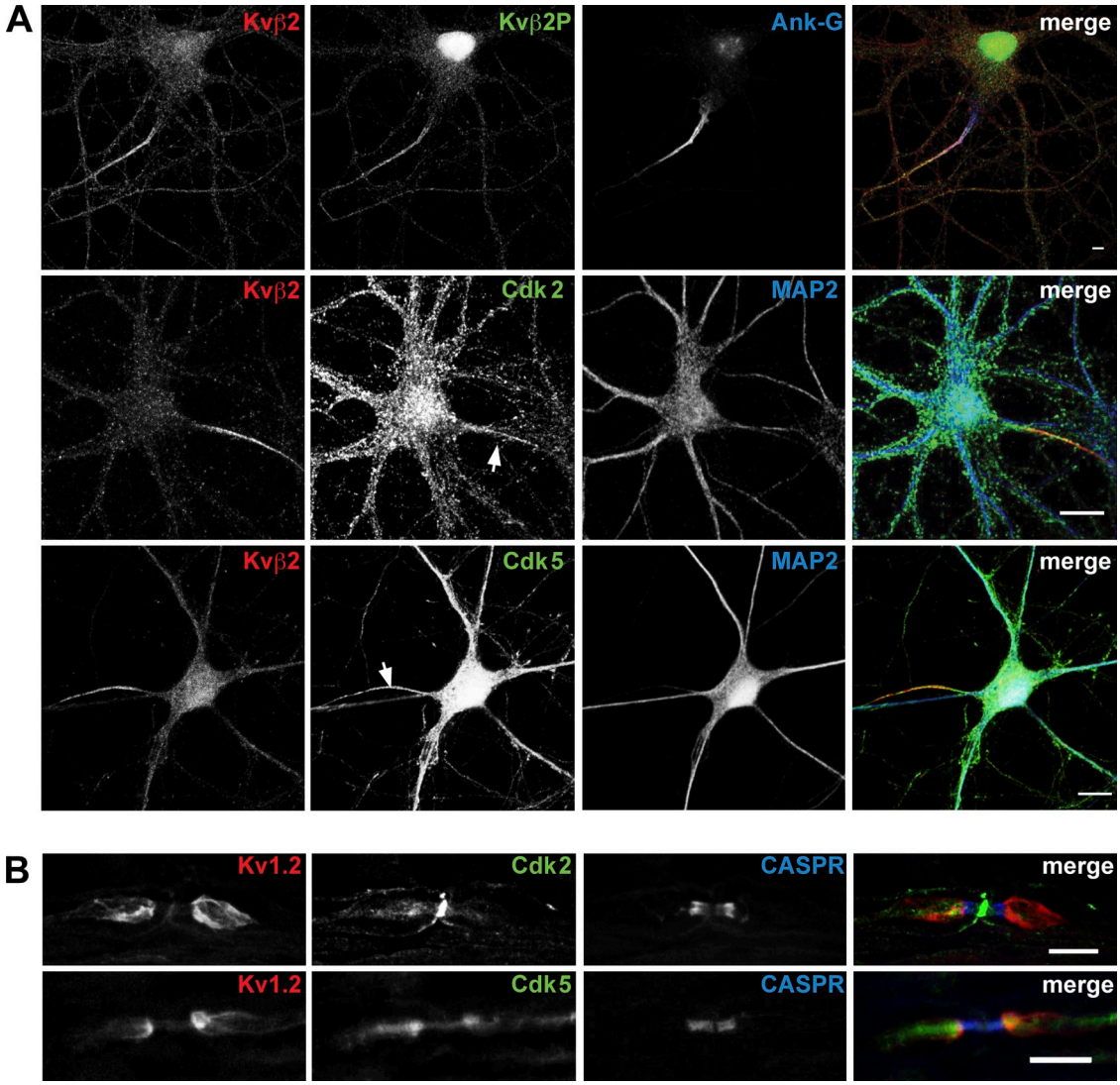

Figure 5. **Localization of endogenous Cdks, Kvβ2, and Kv1.2 in dissociated hippocampal neurons and in sciatic nerve.** (A) Endogenous neuronal Kvβ2 phosphorylated at S31, Cdk2, and Cdk5 are distributed along the axon with enrichment at the AIS. Cultured hippocampal neurons (21 DIV for Kvβ2P and Cdk2; 16 DIV for Cdk5) immunostained with phosphospecific Ab Kvβ2P, anti-Kvβ2 mAb K25/73, and either anti-Cdk2 or anti-Cdk5 Abs. MAP2 immunostaining reveals the somatodendritic compartment and Ank-G immunostaining marks the AIS (arrows). Bars: 8 µm (top), 20 µm (middle), 10 µm (bottom). (B) Immunohistochemistry of adult mouse sciatic nerve. Immunostaining for Cdk2 is distributed at the node of Ranvier and at the juxtaparanode where it colocalizes with Kv1.2. Cdk5 immunostaining is enriched at the juxtaparanode, and is present at paranode and at the node of Ranvier. CASPR immunostaining marks the paranodal compartment. Bar, 10 µm.

was also found enriched at the juxtaparanode in sciatic nerve axons, where it colocalized with Kv1.2 immunostaining, and was also found at the node of Ranvier and at the paranode (Fig. 5 B). Together, these observations demonstrate that axonal Cdk2 and Cdk5 localize at sites of high densities of Kv1–Kvβ2 complexes in dissociated hippocampal neurons and in sciatic nerves, and show that these Cdks are at locations where they can impact phosphorylation-dependent targeting of channel complexes into the axonal membrane.

Cdk inhibitors modulate the endogenous localization of Kvβ2, EB1, and Kv1 channels

Finally, we tested the impact of pharmacological inhibition of Cdks on the axonal localization of endogenous neuronal EB1, Kvβ2, and Kv1α subunits. We treated cultured hippocampal neurons at 20 DIV for 24 h with roscovitine. Because Kv1α subunits, Kvβ2, Cdk2, Cdk5, and EB1 (Fig. S3) are all concentrated at the AIS, we analyzed the effects of Cdk inhibition on their AIS localization. Immunofluorescence staining intensity was quantified by taking the ratio of average fluorescence intensity for the AIS, as defined by immunostaining for Ank-G, relative to that on dendrites. In roscovitine-treated neurons, the immunostaining for Kvβ2, EB1, Kv1.1, and Kv1.2 at the AIS was increased by an average of 30% compared with control (untreated) neurons (n = 50, three independent experiments; Fig. 6, A and B). The increase in Kvβ2 and Kv1.2 immunostaining after roscovitine treatment was also observed in proximal (adjacent to the AIS) and distal axonal domains (Fig. S4). However, the level of PSD-93, a scaffolding protein critical to anchoring of Kv1 channels at the AIS (Ogawa et al., 2008), was

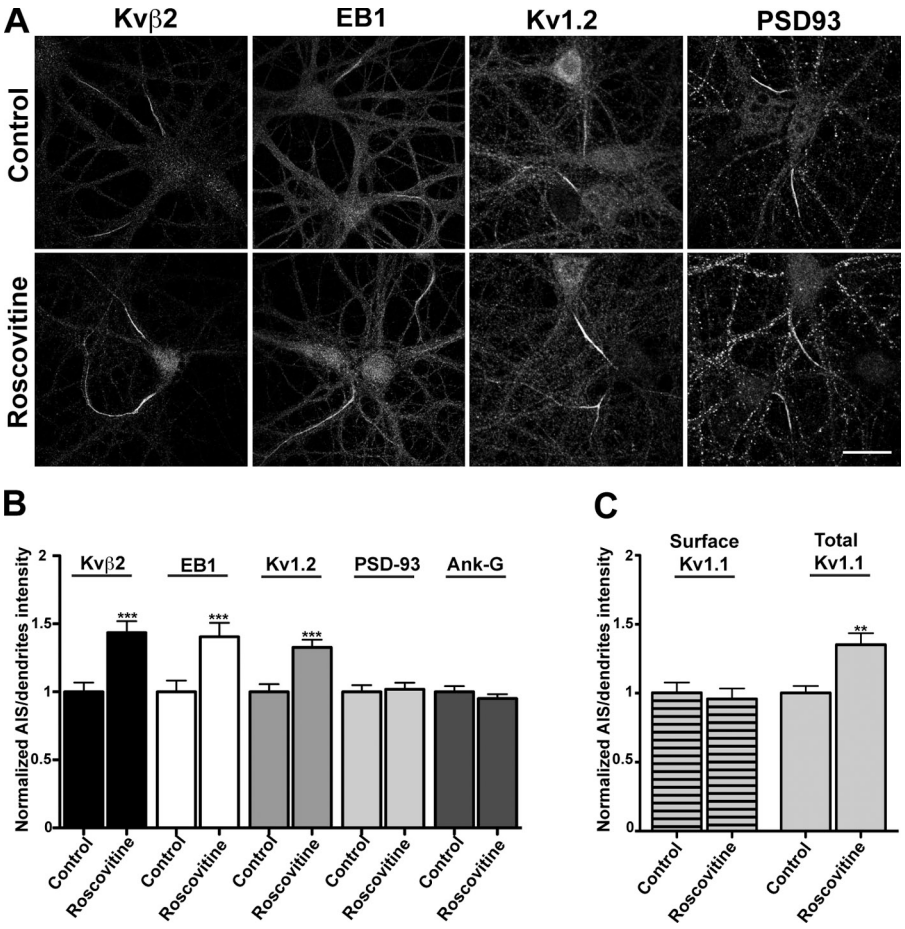

Figure 6. **Effect of Cdk inhibition on the AIS localization of Kvβ2, EB1, Kv1α subunits, PSD-93, and Ank-G.** (A) Cultured hippocampal neurons (21 DIV), with or without 10 µM roscovitine treatment for 24 h, were multiple immunofluorescence stained for Kvβ2, EB1, Kv1.2, and PSD-93 as noted, together with Ank-G as a specific marker of the AIS. Bar, 20 µm. (B) The changes in AIS accumulation were quantified by the ratio of average fluorescent intensity for the AIS to dendritic branches using NIH Neuron/J and subjected to statistical analysis using PRISM 5 (n = 60). ***, $P < 0.001$. (C) Intact neurons were immunostained with Kv1.1e mAb K36/15, and then permeabilized and immunostained with anti-Kv1.1 and anti-Ank-G Abs. Surface axonal polarity index was determined by quantifying the surface immunofluorescence intensity profiles of the AIS versus three dendritic branches using NIH Neuron/J and subjected to statistical analysis using PRISM 5 (n = 25). **, $P < 0.01$.

not affected by roscovitine treatments. To extend these findings, we quantified levels of endogenous cell surface Kv1.1 subunits at the AIS in untreated and roscovitine-treated neurons, using an ectodomain-directed anti-Kv1.1 Ab. Our results showed that the levels of Kv1.1 present at the surface of the AIS remained the same after 24 h of Cdk inhibition (Fig. 6 C). Together, these findings reveal that in neurons the inhibition of Cdks also increases the concentration of EB1 at the AIS, as well as the intracellular populations of Kv1–Kvβ2 channel complexes, implying an accumulation of these proteins on axonal MTs. Together with our previous results in COS-1 cells (see Fig. 4, D and E), this strongly suggests that Cdks modulate the balance between the pool of intracellular Kv1–Kvβ2 complexes associated with MTs via a phosphorylation-sensitive Kvβ2–EB1 interaction, and the pool of plasma membrane Kv1–Kvβ2 complexes associated with PSD-93.

Discussion

It has become clear that Kv1 channels present at the axon, especially at the AIS (Clark et al., 2009) and the juxtaparanode (Rasband, 2004), play a crucial role in controlling spike threshold, shape, and repetitive firing (Johnston et al., 2010). As such, these channels have become an attractive target for therapeutics aimed at restoring function in patients with peripheral demyelinating disorders (Judge et al., 2006). However, the molecular mechanisms responsible for their precise, high density accumulation at these sites remain elusive, but presumably involve reversible protein–protein interactions between component subunits of the Kv1 channel complex and constituents of the neuronal trafficking machinery. In this study, we reveal a novel mechanism regulating axonal targeting of Kv1 channels via the Cdk-mediated phosphorylation of the Kvβ2 auxiliary subunit. Our data suggest a model whereby phosphorylation of Kvβ2 disrupts its binding to EB1, which consequently releases the Kv1–Kvβ2-containing vesicles from their association with EB1 and axonal MTs. We first identified in vivo phosphosites on Kvβ2 purified from mammalian brain using a phosphoproteomic approach. We demonstrated that mutation of two of the identified phosphosites, at S9 and S31, impacts Kvβ2–EB1 interaction, and that Cdk-mediated Kvβ2 phosphorylation negatively regulates this interaction. Furthermore, we showed that Cdk2 and Cdk5 directly phosphorylate Kvβ2 in vitro, and that inhibition of Cdks in heterologous cells leads to an increase of Kvβ2 recruitment on MTs and a decrease of Kv1 surface expression. We found that endogenous Cdk2, Cdk5, phosphorylated Kvβ2, and EB1 in cultured hippocampal neurons are all present in axons, and that all are enriched at the AIS. Cdk2 and Cdk5 also colocalize with Kv1 channels at the juxtaparanode of sciatic nerves in vivo. Finally, acute inhibition of Cdks in cultured hippocampal neurons leads to an increase in the levels of intracellular populations of axonal Kvβ2, EB1, and Kv1 channels without affecting the levels of either the surface population of Kv1 channels or the Kv1 channel anchoring protein PSD-93.

Together, our findings reveal a new regulatory mechanism for the targeting of Kv1 complexes to the axonal membrane through the reversible phosphorylation-dependent binding of Kvβ2 auxiliary subunits to EB1.

Here, we show that two Ser residues, S9 and S31, regulate the interaction of Kvβ2 with EB1, in that phosphorylation or mutation of either Ser residue disrupts Kvβ2–EB1 interaction. The S9 and S31 sites (SPAR and SPKR) are quite similar to a phosphosite (SPRK) that acts as a negative regulator of APC binding to EB1 (Honnappa et al., 2005, 2009). These Kvβ2 phosphosites are located within the Kvβ2 N-terminal domain that among Kvβ subunits is unique to Kvβ2, suggesting that, among Kvβ family members, the reversible binding to EB1 may be specific to the highly expressed Kvβ2. Honnappa et al. (2009) also identified a highly conserved "microtubule tip localization signal" among EB1-binding partners, in the form of a short peptide motif Ser-X-Ile-Pro (SXIP) that targets these partners to growing MT ends in an EB1-dependent manner. Phosphorylation of +TIPs at regulatory sites distinct from but near the SXIP EB1 binding motif negatively regulates the localization of +TIPs to MT ends by decreasing their affinity for binding to EB1 (Honnappa et al., 2005, 2009). However, phosphorylation within the SXIP motif itself has not been detected (Honnappa et al., 2009). There exists a consensus SXIP motif within Kvβ2 (SGIP, aa 257–260), within a segment that among Kvβ subunits is also unique to Kvβ2, and that within the Kvβ2 crystal structure forms a surface loop between the β1 strand and the αG helix (Gulbis et al., 1999, 2000). However, we found that mutating either S257 or the entire SGIP motif to Ala did not abrogate Kvβ2–EB1 interaction (Fig. S5). This suggests that Kvβ2 possesses a mechanism for phosphorylation-dependent interaction with EB1 that is similar to but distinct from other EB1-binding proteins.

Moreover, although our results show a role for N-terminal Kvβ2 phosphorylation acting as a negative regulator of binding to EB1, they are distinct from those obtained for phosphorylation-dependent regulation of EB1 binding by CLASPs (Kumar et al., 2009; Watanabe et al., 2009). For example, Ser to Ala mutations in CLASPs yield constitutive CLASP/EB1 binding that is refractory to phosphorylation-dependent regulation. Similar mutations in Kvβ2 disrupt its binding to EB1, as do Ser to Asp mutations at these sites. We note that there are numerous cases where Ser to Ala mutations are disruptive to other protein–protein interactions that are negatively regulated by phosphorylation. For example, while phosphorylation of GluR2 glutamate receptor subunit at S880 negatively regulates GluR2 binding to its partner GRIP (Matsuda et al., 1999), mutation of S880 to either Ala (Osten et al., 2000) or Glu (Chung et al., 2000) disrupts this interaction, suggesting a similar requirement for an intact, unphosphorylated Ser for binding. Similarly, Kir2.3 channel binding to the PSD-95 scaffolding protein is negatively regulated by phosphorylation at Kir2.3 S440, and by mutation of this Ser to Ala, Asp, or Glu (Cohen et al., 1996). The negative effects of phosphorylation, and of S9 and S31 mutations on Kvβ2 binding to EB1, may reflect a similar strict requirement for an unphosphorylated Ser at these positions.

In neurons, Kvβ2 orchestrates forward trafficking (Shi et al., 1996; Campomanes et al., 2002; Gu et al., 2003) and subsequent axonal targeting (Gu et al., 2003) of Kv1 channels through interactions with EB1 and the microtubule-based motors KIF3A (Gu et al., 2006). KIF5B has also been shown to be required for efficient targeting of Kv1 channels to axons (Rivera et al., 2007), but any potential Kvβ2–KIF5B interaction has not yet been characterized. One model derived from these studies is that Kvβ2 acts as an adaptor protein, linking Kv1-containing vesicles to these motor proteins. As such, Kvβ2 interaction with KIF3 (and possibly KIF5B), which likely occurs after Kv1-containing vesicles exit the Golgi apparatus, allows these vesicles to be transported to the axon along MTs. Once KIF-driven vesicles containing Kv1–Kvβ2 complexes reach the plus end of MTs that are distributed distally along the axon, the Kvβ2 adaptor, and the associated Kv1-containing vesicles, can switch from binding these motors to binding EB1. The newly established Kvβ2–EB1 binding then allows the vesicles to either stay bound to the MTs, by shifting between different MTs in the bundle, or to be released to be locally inserted into the plasma membrane. Here, we found that Cdk phosphorylation inhibits Kvβ2 interaction with EB1, and that pharmacological inhibition of Cdks increases the recruitment of Kvβ2 to MTs in heterologous cells, and the concentration of Kv1–Kvβ2 complexes associated with EB1 in axons. Thus, it is tempting to propose that Cdks play a key role in promoting the release of Kv1–Kvβ2-containing vesicles from EB1. Such a scenario is consistent with previous studies showing that the unloading and transport efficiencies of other cargos are regulated by phosphorylation events (Sato-Yoshitake et al., 1992; Morfini et al., 2002; Guillaud et al., 2008). Therefore, the phosphorylation of Kvβ2 by Cdks would act as a molecular switch that controls the release of Kv1-containing vesicles. We showed that Cdk inhibition decreases the Kv1 channel surface pool in heterologous cells and has no significant effect on the Kv1 surface pool and its anchoring protein PSD-93 in neurons. However, the inhibition of Cdks in heterologous cells was done at the outset of Kv1–Kvβ2 expression, in contrast to the experiments in neurons, where these channel complexes were already transported to and concentrated at the plasma membrane. Moreover, previous studies showed that the axonal Kv1 complexes anchored by PSD-93 at the plasma membrane are highly stable (Ogawa et al., 2008), and that PSD-93 interacts with Kv1 complexes only when they are at the cell surface. Thus, it is likely that 24 h of Cdk inhibition is not long enough to induce a decrease of the concentration of either surface Kv1 channels or PSD-93 at the AIS.

The reversible posttranslational modification of neuronal protein binding partners is a key process allowing a specific and dynamic network of interactions in response to neuronal activity. This process relies on the expression and activity of specific sets of protein kinases and phosphatases in distinct subcellular compartments. Here, we show that neuronal Cdks, which colocalize in axons with Kv1 subunits, Kvβ2, and EB1, are implicated in regulating Kv1 channel axonal compartmentalization. Thus, it is likely that the localization of Cdks at/near sites of high densities of axonal Kv1 channels spatially restricts where the phosphorylation events that regulate Kvβ2–EB1 occur.

This ensures that Kv1 channels are localized at the correct subcellular locations, and prevents their ectopic expression at sites that could result in deranged neuronal excitability. This is similar to the role proposed for the CK2 protein kinase, which is also highly enriched at the AIS and at nodes of Ranvier, and which regulates the local interaction between Nav channels and the scaffolding protein Ank-G (Bréchet et al., 2008). In this case, CK2-mediated phosphorylation increases the affinity of the Nav1 AIS-targeting motif for binding to Ank-G, ensuring that Nav channels are spatially restricted to sites (e.g., the AIS and nodes of Ranvier) that are enriched in Ank-G. The initiation of action potentials depends on the precise density of Nav and Kv channels at the AIS (Clark et al., 2009). Fine tuning of the expression levels and localization of these axonal ion channels, through feedback mechanisms involving signaling pathways using the CK2 and Cdk protein kinases, and competing protein phosphatases, provides a powerful mechanism to dynamically regulate the biophysical properties of the spike-generating machinery and neuronal excitability.

Materials and methods

Preparation of brain membrane fractions and cell lysates
A crude synaptosomal membrane fraction was prepared from freshly dissected adult rat or mouse brain, or from human hippocampal tissue from anonymous donors (the Brain and Tissue Bank for Developmental Disorders at the University of Maryland, Baltimore, MD) by homogenization in 0.3 M sucrose, 5 mM sodium phosphate, pH 7.4, 5 mM NaF, 1 mM EDTA, anti-protease tablet (Roche), and centrifugations as described previously (Trimmer, 1991). The pellet of the crude membranes was suspended in the homogenization buffer and protein was determined using the BCA (bicinchoninic acid protein assay) method (Thermo Fisher Scientific). Harvested HEK293 and COS-1 cells or crude synaptosomal membrane were lysed in 1% Triton X-100 extraction buffer as described previously (Vacher et al., 2007). Cells were transiently transfected using the Lipofectamine 2000 (Invitrogen) or Polyfect (QIAGEN) reagents using the manufacturer's protocols.

Immunopurification, in-gel digestion, and MS
For large-scale immunopurification, 1% Triton X-100 extracts of rat brain membranes (RBM; 25 mg), mouse brain membranes (MBM; 10 mg), or human hippocampal membranes (10 mg) were incubated with affinity-purified rabbit anti-Kv1.2C polyclonal Ab (Rhodes et al., 1995), followed by binding to protein A–agarose beads. In-gel digestion of the Kvβ2 band excised from a Coomassie blue–stained SDS gel was performed in 10 ng/ml trypsin as described previously (Park et al., 2006). An ultra-performance liquid chromatography system (nanoACQUITY; Waters) directly coupled with an ion trap mass spectrometer (LTQ-FT; Finnigan) was used for LC-MS/MS data acquisition. MS/MS spectra were interpreted through the Mascot searches (Matrix Science) with a mass tolerance of 20 ppm, MS/MS tolerance of 0.4 or 0.6 D, and one missing cleavage site allowed. Carbamidomethylation of cysteine, oxidation of methionine, and phosphorylation on serine, threonine, and tyrosine residues was allowed. Each filtered MS/MS spectrum exhibiting possible phosphorylation was manually checked and validated. Existence of a 98-D mass loss ($-H_3PO_4$: phosphopeptide-specific CID neutral loss) and any ambiguity of phosphosites were carefully examined (Park et al., 2006). All LC-MS/MS procedures were performed at the UC Davis Proteomics Facility.

Recombinant protein expression and purification
Plasmids encoding GST-EB1c or GST-EB1 were a gift from Gregg G. Gunderson (Columbia University, New York, NY). All GST constructs were transformed into BL21 (DE3) *Escherichia coli*. Transformed bacteria cells were grown and GST proteins purified by chromatography on glutathione–Sepharose 4B according to the manufacturer's instructions (GE Healthcare). Cleavage of GST fusion protein (for GST-Kvβ2 or GST-Kvβ2 mutants) was performed using PreScission protease following the manufacturer's instructions (GE Healthcare). Protein concentrations were determined by the BCA method (Thermo Fisher Scientific).

Immunoprecipitations, immunoblotting, GST pull-downs, and alkaline phosphatase
Procedures for immunoprecipitation and immunoblot analysis were performed as reported previously (Park et al., 2006). Mouse anti-Kvβ2 mAb K25/73, generated against a C-terminal peptide corresponding to Kvβ2 amino acids 350–367 (Rhodes et al., 1995), was used for immunoblots. For GST pull-downs, transfected cell extracts or purified bacterially expressed WT and mutant Kvβ2 isoforms were incubated 4 h to overnight at 4°C with GST-EB1C, GST-EB1, or GST prebound to glutathione–Sepharose 4B (GE Healthcare). The beads were then washed five times with lysis buffer (Vacher et al., 2007) and eluted with reducing sample buffer (125 mM Tris-HCl, 4% SDS, 20%, glycerol, and 2% β-mercaptoethanol). Membrane preparations and cell lysates were incubated without or with 100 U/ml of alkaline phosphatase (Roche) as reported previously (Murakoshi et al., 1997).

In vitro phosphorylation assay
Bacterially expressed GST-Kvβ2 (Bekele-Arcuri et al., 1996) fusion protein (2.5 µg) was incubated with 100 ng of human recombinant Cdk complexes (Invitrogen), either Cdk2/cyclin A, or Cdk5/p35, and 2 mM ATP in kinase reaction buffer (20 mM Tris-HCl, pH 7.5, 1 mM $MgCl_2$, and 1 mM DTT) in a final volume of 50 µl for 15 min at 30°C. The reaction was stopped by adding 50 µl of 2x reducing sample buffer.

Plasmids and generation of mutant Kvβ2 cDNAs
Plasmids for transfection were as follows: rat Kv1.2/RBG4, rat Kvβ2/RBG4 (Nakahira et al., 1996), EB1-EGFP (a gift from Michelle Piehl, Lehigh University, Bethlehem, PA), Cdk2-HA (Addgene plasmid 1884), and Cdk2-DN (D146N, Addgene plasmid 1882; van den Heuvel and Harlow, 1993). Mutagenesis of recombinant rat Kvβ2 cDNA in the pRBG4 or pGEX-6P vectors (Nakahira et al., 1996) was performed using the QuikChange site-directed mutagenesis kit (Agilent Technologies).

Generation of the phosphospecific Ab Kvβ2P
A synthetic peptide phosphorylated at S31 (aa 26–37, STRYG[pS]PKRQLQ) and the nonphosphorylated equivalent peptide were synthesized (Pi Proteomics). The phosphopeptide was conjugated to keyhole limpet hemocyanin (EMD) at a ratio of 1 mg of peptide/mg of carrier protein using sulfo-m-maleimidobenzoyl-NHS ester (Thermo Fisher Scientific), and injected into rabbits for the production of polyclonal antisera (PRF&L). For affinity purification, the phosphorylated and nonphosphorylated peptides were conjugated to SulfoLink coupling gel (Thermo Fisher Scientific) via synthetic N-terminal cysteine residues, and phosphospecific Abs were affinity purified by a two-step affinity purification procedure (Park et al., 2006). Phosphospecificity was verified by ELISA assay against phosphorylated and nonphosphorylated peptide coupled to BSA.

Animals
Wistar rats (for neuronal cultures) and Swiss mice (for sciatic nerve immunohistochemistry) used follow the guidelines established by the European Animal Care and Use Committee (86/609/CEE). Mice were deeply anesthetized with pentobarbital (120 mg/kg b.w., i.p.).

Neuron culture, transfection, and inhibition of Cdk activity
Primary hippocampal neurons were prepared from hippocampi of E18 rats, as described previously (Goslin and Banker, 1989). In brief, dissociated neurons were plated onto poly-L-lysine–treated glass coverslips at a density of 2,500–7,500 cells/cm^2 and co-cultured over a monolayer of astrocytes. Cells were maintained in Neurobasal medium (Invitrogen) supplemented with B27 and glutamine. Neurons were transfected at 7 DIV or at 10 DIV using Lipofectamine 2000 (Invitrogen). The conditioned medium was supplemented with 10 µM D-2-amino-5-phosphonopentanoic acid (Tocris Bioscience). Transfected cells were processed for immunofluorescence 2 d after transfection. Inhibition of Cdk activity was performed using roscovitine (EMD), a potent inhibitor of Cdk1, Cdk2, and Cdk5 (Meijer et al., 1997; Bach et al., 2005). Roscovitine was dissolved in DMSO and added to the culture medium of rat hippocampal neurons at a final concentration of 10 µM for 24 h. Controls included the same amount of DMSO alone.

Immunofluorescence staining
For surface immunofluorescence staining (Tiffany et al., 2000), cells were immunostained 48 h after transfection with ectodomain-directed rabbit polyclonal Kv1.2e Ab (Shi et al., 1996) or, for immunostaining of endogenous neuronal Kv1.1, at 21 DIV with ectodomain-directed mouse Kv1.1e mAb (K36/15; UC Davis/NIH NeuroMab Facility) before detergent permeabilization to detect the cell surface pool. The total cellular pools of the respective proteins were detected by immunostaining with cytoplasmically

directed mouse mAbs K14/16 (anti-Kv1.2) or K20/78 (anti-Kv1.1), all from the UC Davis/NIH NeuroMab Facility, or K25/73 (anti-Kvβ2) after detergent permeabilization. For immunostaining endogenous neuronal targets, rat hippocampal neurons were incubated for 1 h with these mAbs and mouse anti-Ank-G mAb (N106/36 or N106/65), or mouse anti-PSD-93 (N18/30) all from the UC Davis/NIH NeuroMab Facility; rat anti-EB1 mAb (KT-51; AbCam); or rabbit anti-Cdk2 or anti-Cdk5 (H-298 and C-8, respectively; Santa Cruz Biotechnology, Inc.). Corresponding species- or mouse isotype–specific secondary Abs conjugated to Alexa Fluor 488, 555, and 633 or Cy5 (Invitrogen) were incubated for 1 h. Coverslips were mounted in FluorSave reagent (EMD). Cells were imaged using a confocal microscope (TCS-SPE or TSC-SP2; LAS-AF software; Leica). Confocal images were acquired with 40×/1.25 NA and 63×/1.40 NA oil objectives (Leica) at room temperature. Fluorescence was collected as Z stacks with sequential wavelength acquisition. Quantification was performed using ImageJ software (National Institutes of Health, Bethesda, MD). Regions of interest corresponding to AIS were manually selected on ankG images and reported on other channels for intensity measurements. All intensities were corrected for background labeling. For illustration, image editing was performed using ImageJ or Photoshop CS3 (Adobe) and was limited to rolling-ball background subtraction, linear-contrast enhancement. For immunohistochemistry, sciatic nerves were removed, fixed in 4% paraformaldehyde for 10 min, and then cryoprotected using sucrose gradient before being frozen. Several cryostat sections of 12-µm and 25-µm thickness were made. The sections were blocked with 50 µg/ml BSA, 0.5% Triton X-100, 1% normal goat serum, and 1% normal donkey serum in PBS for 90 min. They were incubated overnight at 4°C with primary Abs in 10 µg/ml BSA, 0.1% normal goat serum, and 0.1% normal donkey serum in PBS, then with secondary Abs in the same buffer for 1 h. In some preparations, 0.1 µM DAPI nucleic acid stain (Invitrogen) was added for 10 min before mounting with FluorSave.

Electrophysiology

Outward potassium currents were recorded at room temperature from HEK293 cells transiently coexpressing recombinant Kv1.2 with WT or mutant Kvβ2 using whole-cell voltage-clamp configuration. Patch pipettes were pulled from borosilicate glass tubing (TW150F; World Precision Instruments, Inc.) to give a resistance of 1–3 mΩ when filled with pipette solution. Currents were recorded with an EPC-10 patch-clamp amplifier (HEKA), sampled at 10 kHz, and filtered at 2 kHz using a digital Bessel filter. All currents were capacitance- and series-resistance compensated, and leak-subtracted by standard *P/n* procedure. Current recordings were done with continuous superfusion of extracellular buffer, which contained (mM): 140 NaCl, 5 KCl, 2 $CaCl_2$, 2 $MgCl_2$, 10 glucose, and 10 Hepes, pH 7.3. Pipette solution contained (mM): 140 KCl, 2 $MgCl_2$, 1 $CaCl_2$, 5 EGTA, 10 glucose, and 10 Hepes, pH 7.3. For steady-state activation experiments, cells were held at −100 mV and step depolarized to +80 mV for 200 ms with depolarizing 10-mV increments. For steady-state inactivation experiments, cells were held at −100 mV and step depolarized to +40 mV (test pulse) for 10 s with 10-mV increments (conditioning steady pulse) followed by a test pulse at +10 mV. The inter-pulse interval was 10 s. Current density was determined by dividing peak current amplitude at each test potential by cell capacitance, and was plotted against respective test potentials. PULSE software (HEKA) was used for acquisition and analysis of currents. IGOR Pro 4 (WaveMetrix, Inc.), and Origin 7 software (OriginLab Corporation) were used to perform least squares fitting and to create figures.

Online supplemental material

Fig. S1 shows the phosphorylation of Kvβ2 in heterologous cells and in mammalian brain. Fig. S2 shows the effect of Kvβ2 S9A/S31A mutant on endogenous Kv1.2 axonal distribution. Fig. S3 shows the subcellular distribution of EB1 in cultured hippocampal neurons at 21 DIV. Fig. S4 shows the effect of Cdk inhibition on Kv1 channel and Kvβ2 distribution in proximal and distal axons. Fig. S5 shows the effect of the mutagenesis of Kvβ2 SGIP motif on its interaction with EB1. Online supplemental material is available at http://www.jcb.org/cgi/content/full/jcb.201007113/DC1.

We thank Stephanie Angles-d'Ortoli, Ghislaine Caillol, Fanny Rueda, and Norma Villalon for expert technical assistance; Dr. Gregg G. Gundersen for providing the GST-EB1 constructs; Dr. Sander van den Heuvel for Cdk plasmids; Dr. Kang Sik-Park and Dr. Frank Berendt for their assistance in mass spectrometry; and Dr. Christophe Leterrier for his helpful comments and NIH Neuron/J macros.

This work was supported by NIH grant NS34383 (to J.S. Trimmer), the Institut National de la Santé et de la Recherche Médicale, Marie Curie seventh framework program grant IRG-2008-239499 (to H. Vacher), a Fondation pour la Recherche Médicale grant (to B. Dargent), and a postdoctoral fellowship (to H. Vacher). We also thank the Centre National de la Recherche Scientifique for additional financial support (to H. Vacher and B. Dargent).

Submitted: 20 July 2010
Accepted: 1 February 2011

References

Adelman, J.P., C.T. Bond, M. Pessia, and J. Maylie. 1995. Episodic ataxia results from voltage-dependent potassium channels with altered functions. *Neuron*. 15:1449–1454. doi:10.1016/0896-6273(95)90022-5

Bach, S., M. Knockaert, J. Reinhardt, O. Lozach, S. Schmitt, B. Baratte, M. Koken, S.P. Coburn, L. Tang, T. Jiang, et al. 2005. Roscovitine targets, protein kinases and pyridoxal kinase. *J. Biol. Chem.* 280:31208–31219. doi:10.1074/jbc.M500806200

Baek, J.H., O. Cerda, and J.S. Trimmer. 2011. Mass spectrometry-based phosphoproteomics reveals multisite phosphorylation on mammalian brain voltage-gated sodium and potassium channels. *Semin. Cell Dev. Biol.* In press.

Bean, B.P. 2007. The action potential in mammalian central neurons. *Nat. Rev. Neurosci.* 8:451–465. doi:10.1038/nrn2148

Bekele-Arcuri, Z., M.F. Matos, L. Manganas, B.W. Strassle, M.M. Monaghan, K.J. Rhodes, and J.S. Trimmer. 1996. Generation and characterization of subtype-specific monoclonal antibodies to K+ channel alpha- and beta-subunit polypeptides. *Neuropharmacology*. 35:851–865. doi:10.1016/0028-3908(96)00128-1

Bieling, P., L. Laan, H. Schek, E.L. Munteanu, L. Sandblad, M. Dogterom, D. Brunner, and T. Surrey. 2007. Reconstitution of a microtubule plus-end tracking system in vitro. *Nature*. 450:1100–1105. doi:10.1038/nature06386

Bréchet, A., M.P. Fache, A. Brachet, G. Ferracci, A. Baude, M. Irondelle, S. Pereira, C. Leterrier, and B. Dargent. 2008. Protein kinase CK2 contributes to the organization of sodium channels in axonal membranes by regulating their interactions with ankyrin G. *J. Cell Biol.* 183:1101–1114. doi:10.1083/jcb.200805169

Campomanes, C.R., K.I. Carroll, L.N. Manganas, M.E. Hershberger, B. Gong, D.E. Antonucci, K.J. Rhodes, and J.S. Trimmer. 2002. Kv beta subunit oxidoreductase activity and Kv1 potassium channel trafficking. *J. Biol. Chem.* 277:8298–8305. doi:10.1074/jbc.M110276200

Chung, Y.H., C.M. Shin, M.J. Kim, and C.I. Cha. 2000. Immunohistochemical study on the distribution of six members of the Kv1 channel subunits in the rat basal ganglia. *Brain Res.* 875:164–170. doi:10.1016/S0006-8993(00)02586-5

Clark, B.D., E.M. Goldberg, and B. Rudy. 2009. Electrogenic tuning of the axon initial segment. *Neuroscientist*. 15:651–668. doi:10.1177/1073858409341973

Cohen, N.A., J.E. Brenman, S.H. Snyder, and D.S. Bredt. 1996. Binding of the inward rectifier K+ channel Kir 2.3 to PSD-95 is regulated by protein kinase A phosphorylation. *Neuron*. 17:759–767. doi:10.1016/S0896-6273(00)80207-X

Dixit, R., B. Barnett, J.E. Lazarus, M. Tokito, Y.E. Goldman, and E.L. Holzbaur. 2009. Microtubule plus-end tracking by CLIP-170 requires EB1. *Proc. Natl. Acad. Sci. USA*. 106:492–497. doi:10.1073/pnas.0807614106

Goldberg, E.M., B.D. Clark, E. Zagha, M. Nahmani, A. Erisir, and B. Rudy. 2008. K+ channels at the axon initial segment dampen near-threshold excitability of neocortical fast-spiking GABAergic interneurons. *Neuron*. 58:387–400. doi:10.1016/j.neuron.2008.03.003

Goslin, K., and G. Banker. 1989. Experimental observations on the development of polarity by hippocampal neurons in culture. *J. Cell Biol.* 108:1507–1516. doi:10.1083/jcb.108.4.1507

Gu, C., Y.N. Jan, and L.Y. Jan. 2003. A conserved domain in axonal targeting of Kv1 (Shaker) voltage-gated potassium channels. *Science*. 301:646–649. doi:10.1126/science.1086998

Gu, C., W. Zhou, M.A. Puthenveedu, M. Xu, Y.N. Jan, and L.Y. Jan. 2006. The microtubule plus-end tracking protein EB1 is required for Kv1 voltage-gated K+ channel axonal targeting. *Neuron*. 52:803–816. doi:10.1016/j.neuron.2006.10.022

Guillaud, L., R. Wong, and N. Hirokawa. 2008. Disruption of KIF17-Mint1 interaction by CaMKII-dependent phosphorylation: a molecular model of kinesin-cargo release. *Nat. Cell Biol.* 10:19–29. doi:10.1038/ncb1665

Gulbis, J.M., S. Mann, and R. MacKinnon. 1999. Structure of a voltage-dependent K+ channel beta subunit. *Cell*. 97:943–952. doi:10.1016/S0092-8674(00)80805-3

Gulbis, J.M., M. Zhou, S. Mann, and R. MacKinnon. 2000. Structure of the cytoplasmic beta subunit-T1 assembly of voltage-dependent K+ channels. *Science*. 289:123–127. doi:10.1126/science.289.5476.123

Honnappa, S., C.M. John, D. Kostrewa, F.K. Winkler, and M.O. Steinmetz. 2005. Structural insights into the EB1-APC interaction. *EMBO J.* 24:261–269. doi:10.1038/sj.emboj.7600529

Honnappa, S., S.M. Gouveia, A. Weisbrich, F.F. Damberger, N.S. Bhavesh, H. Jawhari, I. Grigoriev, F.J. van Rijssel, R.M. Buey, A. Lawera, et al. 2009. An EB1-binding motif acts as a microtubule tip localization signal. *Cell*. 138:366–376. doi:10.1016/j.cell.2009.04.065

Inda, M.C., J. DeFelipe, and A. Muñoz. 2006. Voltage-gated ion channels in the axon initial segment of human cortical pyramidal cells and their relationship with chandelier cells. *Proc. Natl. Acad. Sci. USA*. 103:2920–2925. doi:10.1073/pnas.0511197103

Jen, J.C., T.D. Graves, E.J. Hess, M.G. Hanna, R.C. Griggs, and R.W. Baloh; CINCH investigators. 2007. Primary episodic ataxias: diagnosis, pathogenesis and treatment. *Brain*. 130:2484–2493. doi:10.1093/brain/awm126

Johnston, J., I.D. Forsythe, and C. Kopp-Scheinpflug. 2010. Going native: voltage-gated potassium channels controlling neuronal excitability. *J. Physiol.* 588:3187–3200. doi:10.1113/jphysiol.2010.191973

Judge, S.I., J.M. Lee, C.T. Bever Jr., and P.M. Hoffman. 2006. Voltage-gated potassium channels in multiple sclerosis: Overview and new implications for treatment of central nervous system inflammation and degeneration. *J. Rehabil. Res. Dev.* 43:111–122. doi:10.1682/JRRD.2004.09.0116

Kullmann, D.M., and M.G. Hanna. 2002. Neurological disorders caused by inherited ion-channel mutations. *Lancet Neurol.* 1:157–166. doi:10.1016/S1474-4422(02)00071-6

Kumar, P., K.S. Lyle, S. Gierke, A. Matov, G. Danuser, and T. Wittmann. 2009. GSK3beta phosphorylation modulates CLASP-microtubule association and lamella microtubule attachment. *J. Cell Biol.* 184:895–908. doi:10.1083/jcb.200901042

Long, S.B., E.B. Campbell, and R. Mackinnon. 2005. Crystal structure of a mammalian voltage-dependent Shaker family K+ channel. *Science*. 309:897–903. doi:10.1126/science.1116269

Lorincz, A., and Z. Nusser. 2008. Cell-type-dependent molecular composition of the axon initial segment. *J. Neurosci.* 28:14329–14340. doi:10.1523/JNEUROSCI.4833-08.2008

Matsuda, S., S. Mikawa, and H. Hirai. 1999. Phosphorylation of serine-880 in GluR2 by protein kinase C prevents its C terminus from binding with glutamate receptor-interacting protein. *J. Neurochem.* 73:1765–1768. doi:10.1046/j.1471-4159.1999.731765.x

Meijer, L., A. Borgne, O. Mulner, J.P. Chong, J.J. Blow, N. Inagaki, M. Inagaki, J.G. Delcros, and J.P. Moulinoux. 1997. Biochemical and cellular effects of roscovitine, a potent and selective inhibitor of the cyclin-dependent kinases cdc2, cdk2 and cdk5. *Eur. J. Biochem.* 243:527–536. doi:10.1111/j.1432-1033.1997.t01-2-00527.x

Mi, H., T.J. Deerinck, M.H. Ellisman, and T.L. Schwarz. 1995. Differential distribution of closely related potassium channels in rat Schwann cells. *J. Neurosci.* 15:3761–3774.

Morfini, G., G. Szebenyi, R. Elluru, N. Ratner, and S.T. Brady. 2002. Glycogen synthase kinase 3 phosphorylates kinesin light chains and negatively regulates kinesin-based motility. *EMBO J.* 21:281–293. doi:10.1093/emboj/21.3.281

Murakoshi, H., G. Shi, R.H. Scannevin, and J.S. Trimmer. 1997. Phosphorylation of the Kv2.1 K+ channel alters voltage-dependent activation. *Mol. Pharmacol.* 52:821–828.

Nagaya, N., and D.M. Papazian. 1997. Potassium channel alpha and beta subunits assemble in the endoplasmic reticulum. *J. Biol. Chem.* 272:3022–3027. doi:10.1074/jbc.272.5.3022

Nakahira, K., G. Shi, K.J. Rhodes, and J.S. Trimmer. 1996. Selective interaction of voltage-gated K+ channel beta-subunits with alpha-subunits. *J. Biol. Chem.* 271:7084–7089. doi:10.1074/jbc.271.12.7084

Nakahira, K., M.F. Matos, and J.S. Trimmer. 1998. Differential interaction of voltage-gated K+ channel beta-subunits with cytoskeleton is mediated by unique amino terminal domains. *J. Mol. Neurosci.* 11:199–208. doi:10.1385/JMN:11:3:199

Ogawa, Y., I. Horresh, J.S. Trimmer, D.S. Bredt, E. Peles, and M.N. Rasband. 2008. Postsynaptic density-93 clusters Kv1 channels at axon initial segments independently of Caspr2. *J. Neurosci.* 28:5731–5739. doi:10.1523/JNEUROSCI.4431-07.2008

Orlova, E.V., M. Papakosta, F.P. Booy, M. van Heel, and J.O. Dolly. 2003. Voltage-gated K+ channel from mammalian brain: 3D structure at 18A of the complete (alpha)4(beta)4 complex. *J. Mol. Biol.* 326:1005–1012. doi:10.1016/S0022-2836(02)00708-8

Osten, P., L. Khatri, J.L. Perez, G. Köhr, G. Giese, C. Daly, T.W. Schulz, A. Wensky, L.M. Lee, and E.B. Ziff. 2000. Mutagenesis reveals a role for ABP/GRIP binding to GluR2 in synaptic surface accumulation of the AMPA receptor. *Neuron*. 27:313–325. doi:10.1016/S0896-6273(00)00039-8

Park, K.S., D.P. Mohapatra, H. Misonou, and J.S. Trimmer. 2006. Graded regulation of the Kv2.1 potassium channel by variable phosphorylation. *Science*. 313:976–979. doi:10.1126/science.1124254

Pongs, O., T. Leicher, M. Berger, J. Roeper, R. Bähring, D. Wray, K.P. Giese, A.J. Silva, and J.F. Storm. 1999. Functional and molecular aspects of voltage-gated K+ channel beta subunits. *Ann. N. Y. Acad. Sci.* 868:344–355. doi:10.1111/j.1749-6632.1999.tb11296.x

Rasband, M.N. 2004. It's "juxta" potassium channel! *J. Neurosci. Res.* 76:749–757. doi:10.1002/jnr.20073

Rasband, M.N., J.S. Trimmer, T.L. Schwarz, S.R. Levinson, M.H. Ellisman, M. Schachner, and P. Shrager. 1998. Potassium channel distribution, clustering, and function in remyelinating rat axons. *J. Neurosci.* 18:36–47.

Rettig, J., S.H. Heinemann, F. Wunder, C. Lorra, D.N. Parcej, J.O. Dolly, and O. Pongs. 1994. Inactivation properties of voltage-gated K+ channels altered by presence of beta-subunit. *Nature*. 369:289–294. doi:10.1038/369289a0

Rhodes, K.J., S.A. Keilbaugh, N.X. Barrezueta, K.L. Lopez, and J.S. Trimmer. 1995. Association and colocalization of K+ channel alpha- and beta-subunit polypeptides in rat brain. *J. Neurosci.* 15:5360–5371.

Rhodes, K.J., M.M. Monaghan, N.X. Barrezueta, S. Nawoschik, Z. Bekele-Arcuri, M.F. Matos, K. Nakahira, L.E. Schechter, and J.S. Trimmer. 1996. Voltage-gated K+ channel beta subunits: expression and distribution of Kv beta 1 and Kv beta 2 in adult rat brain. *J. Neurosci.* 16:4846–4860.

Rhodes, K.J., B.W. Strassle, M.M. Monaghan, Z. Bekele-Arcuri, M.F. Matos, and J.S. Trimmer. 1997. Association and colocalization of the Kvbeta1 and Kvbeta2 beta-subunits with Kv1 alpha-subunits in mammalian brain K+ channel complexes. *J. Neurosci.* 17:8246–8258.

Rivera, J., P.J. Chu, T.L. Lewis Jr., and D.B. Arnold. 2007. The role of Kif5B in axonal localization of Kv1 K(+) channels. *Eur. J. Neurosci.* 25:136–146. doi:10.1111/j.1460-9568.2006.05277.x

Ruppersberg, J.P., K.H. Schröter, B. Sakmann, M. Stocker, S. Sewing, and O. Pongs. 1990. Heteromultimeric channels formed by rat brain potassium-channel proteins. *Nature*. 345:535–537. doi:10.1038/345535a0

Sato-Yoshitake, R., H. Yorifuji, M. Inagaki, and N. Hirokawa. 1992. The phosphorylation of kinesin regulates its binding to synaptic vesicles. *J. Biol. Chem.* 267:23930–23936.

Sewing, S., J. Roeper, and O. Pongs. 1996. Kv beta 1 subunit binding specific for shaker-related potassium channel alpha subunits. *Neuron*. 16:455–463. doi:10.1016/S0896-6273(00)80063-X

Shi, G., K. Nakahira, S. Hammond, K.J. Rhodes, L.E. Schechter, and J.S. Trimmer. 1996. Beta subunits promote K+ channel surface expression through effects early in biosynthesis. *Neuron*. 16:843–852. doi:10.1016/S0896-6273(00)80104-X

Skube, S.B., J.M. Chaverri, and H.V. Goodson. 2010. Effect of GFP tags on the localization of EB1 and EB1 fragments in vivo. *Cytoskeleton (Hoboken)*. 67:1–12.

Sokolova, O., A. Accardi, D. Gutierrez, A. Lau, M. Rigney, and N. Grigorieff. 2003. Conformational changes in the C terminus of Shaker K+ channel bound to the rat Kvbeta2-subunit. *Proc. Natl. Acad. Sci. USA*. 100:12607–12612. doi:10.1073/pnas.2235650100

Tiffany, A.M., L.N. Manganas, E. Kim, Y.P. Hsueh, M. Sheng, and J.S. Trimmer. 2000. PSD-95 and SAP97 exhibit distinct mechanisms for regulating K(+) channel surface expression and clustering. *J. Cell Biol.* 148:147–158. doi:10.1083/jcb.148.1.147

Trimmer, J.S. 1991. Immunological identification and characterization of a delayed rectifier K+ channel polypeptide in rat brain. *Proc. Natl. Acad. Sci. USA*. 88:10764–10768. doi:10.1073/pnas.88.23.10764

Trimmer, J.S. 1998. Regulation of ion channel expression by cytoplasmic subunits. *Curr. Opin. Neurobiol.* 8:370–374. doi:10.1016/S0959-4388(98)80063-9

Vabnick, I., J.S. Trimmer, T.L. Schwarz, S.R. Levinson, D. Risal, and P. Shrager. 1999. Dynamic potassium channel distributions during axonal development prevent aberrant firing patterns. *J. Neurosci.* 19:747–758.

Vacher, H., D.P. Mohapatra, H. Misonou, and J.S. Trimmer. 2007. Regulation of Kv1 channel trafficking by the mamba snake neurotoxin dendrotoxin K. *FASEB J.* 21:906–914. doi:10.1096/fj.06-7229com

van den Heuvel, S., and E. Harlow. 1993. Distinct roles for cyclin-dependent kinases in cell cycle control. *Science*. 262:2050–2054. doi:10.1126/science.8266103

Van Wart, A., J.S. Trimmer, and G. Matthews. 2007. Polarized distribution of ion channels within microdomains of the axon initial segment. *J. Comp. Neurol.* 500:339–352. doi:10.1002/cne.21173

Vitre, B., F.M. Coquelle, C. Heichette, C. Garnier, D. Chrétien, and I. Arnal. 2008. EB1 regulates microtubule dynamics and tubulin sheet closure in vitro. *Nat. Cell Biol.* 10:415–421. doi:10.1038/ncb1703

Wang, H., D.D. Kunkel, T.M. Martin, P.A. Schwartzkroin, and B.L. Tempel. 1993. Heteromultimeric K+ channels in terminal and juxtaparanodal regions of neurons. *Nature*. 365:75–79. doi:10.1038/365075a0

Watanabe, T., J. Noritake, M. Kakeno, T. Matsui, T. Harada, S. Wang, N. Itoh, K. Sato, K. Matsuzawa, A. Iwamatsu, et al. 2009. Phosphorylation of CLASP2 by GSK-3beta regulates its interaction with IQGAP1, EB1 and microtubules. *J. Cell Sci.* 122:2969–2979. doi:10.1242/jcs.046649

Xu, J., W. Yu, J.M. Wright, R.W. Raab, and M. Li. 1998. Distinct functional stoichiometry of potassium channel beta subunits. *Proc. Natl. Acad. Sci. USA*. 95:1846–1851. doi:10.1073/pnas.95.4.1846